Beam-pointing angle calibration of the Wyoming Cloud Radar on the Wyoming King Air aircraft

Samuel Haimov, Alfred Rodi
University of Wyoming, Atmospheric Science Department, Laramie, WY 82071, U.S.A.,
haimov@uwyo.edu

Samuel Haimov

1. Introduction

Atmospheric wind estimation from an airborne weather Doppler radar requires removal of the aircraft motion from the measured radar Doppler velocity. High accuracy estimates of the radar beam pointing angles and measurements of aircraft attitude and velocity are needed for this (Bosart et al., 2002). In this paper, we propose a beam-pointing calibration technique and analyze the errors associated with beam pointing angle determination for the Wyoming Cloud Radar (WCR) on the University of Wyoming King Air (UWKA) research aircraft.

The UWKA is a modified Beechcraft Super King Air 200T equipped with in situ and remote sensing probes for studying atmospheric phenomena in the lower to mid-troposphere (Wang et al., 2012; http://atmos.uwyo.edu/n2uw). The UWKA and WCR are also a part of the United States National Science Foundation Lower Atmospheric Observing Facilities. In the summer of 2011, the UWKA was equipped with a new high-precision geopositioning system from Trimble/Applanix, model POS AV410 (http://www.applanix.com/products/airborne.html). In this study, we post-processed the Inertial Measurement Unit (IMU) linear and angular accelerations measurements with Global Navigation Satellite Systems (GNSS) data to determine the aircraft position, velocity, and attitude angles. Post-processing was done with Applanix POSPac software, implementing a tightly-coupled Kalman filter for the IMU and GNSS data using dual L1/L2 frequency differential techniques. The moment arm effect of the relative IMU-GNSS antenna location was corrected using surveyed locations with better than 0.05 m accuracy. Accuracies estimated by the manufacturer are 0.005 ms^{-1} in velocity, 0.008 degrees in roll and pitch angles and 0.025 degrees in heading.

WCR is a 95 GHz multi-beam Doppler radar capable of utilizing up to 4 "fixed-look" antennas and 5 beam-pointing directions when installed on the UWKA (Wang et al., 2012; http://atmos.uwyo.edu/wcr). In this paper we evaluate the accuracy of the pointing angles of the two WCR down-pointing antennas aligned in the vertical-plane below the aircraft, which are suitable for dual-Doppler wind retrieval (Damiani and Haimov, 2006; Leon at al., 2006). Radar received power and Doppler measurements from a ground surface are utilized in an optimization procedure to estimate the beam pointing angles. Data was collected from variety of aircraft maneuvers flown over relatively flat terrain. Analysis is done to estimate the errors between the inertially-determined and radar-determined velocity along the beam, and the sensitivity to the relative velocity of the IMU and radar antenna caused by aircraft angular acceleration. A simulation of a radar return from a ground surface with a known aircraft motion contribution is performed to evaluate the numerical errors and errors due to optimization inaccuracies.

The result of the calibration procedure is the best estimate of the beam pointing-angles for each antenna, and their uncertainty.

2. The calibration problem

The airborne radar measured Doppler radial velocity from a given radar illuminated volume (hereafter called range gate) can be expressed as $\boldsymbol{v} = \vec{\boldsymbol{b}} \cdot (\vec{\boldsymbol{V}}_{\boldsymbol{s}} + \vec{\boldsymbol{V}}_{\boldsymbol{p}})$. The dot (·) denotes a scalar (inner) product, $\vec{\boldsymbol{V}}_{\boldsymbol{s}}$ is the mean three-dimensional (3-D) velocity vector of the scatterers within the range gate, and $\vec{\boldsymbol{V}}_{\boldsymbol{p}} = (V_{px}, V_{py}, V_{pz})$ is the 3-D velocity vector of the radar platform motion at the radar antenna. $\vec{\boldsymbol{b}} = (b_x, b_y, b_z)$ is the unit vector ($|\vec{\boldsymbol{b}}| = \sqrt{b_x^2 + b_y^2 + b_z^2} = 1$) of the radar beam-pointing vector. The reference coordinate system for the above vectors is the local aircraft reference system (ACRS) **Oxyz**. It is a Cartesian coordinate frame with origin **O** located at the sensing point of the aircraft IMU, **x** is parallel to the aircraft longitudinal axis, **y** is parallel to the aircraft right wing and **z** is pointing down (Fig.1). In the fixed Earth ground coordinate system (FGRS) **O** , the origin **O** is at the Earth's surface below the origin **O** of the ACRS, is East, is North and is up (Fig.1). The representation of the vectors described above in ACRS or FGRS is uniquely defined by a transformation matrix applying known rotations between the coordinate systems. The rotations as given by the Eulerian angles, roll (, about x, right wing down), pitch (θ, about y, nose up), and true heading (, about z, 0˚ being North, positive toward East) are measured by the GNSS/IMU system. After some simple trigonometric derivations (more about mapping between ACRS and FGRS can be found in Lee at al, 1994) the orthogonal transformation matrix from ground coordinate system FGRS to aircraft coordinate system ACRS is:

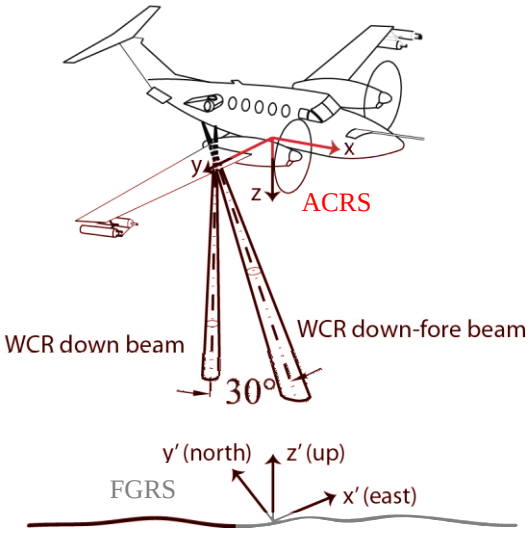

Fig. 1. Schematic presentation of the WCR utilizing two down-pointing antennas on the UWKA.

$$\mathbf{T} = \begin{pmatrix} t_{11} & t_{12} & t_{13} \\ t_{21} & t_{22} & t_{23} \\ t_{31} & t_{32} & t_{33} \end{pmatrix} = \begin{pmatrix} \sin\psi\cos\theta & \cos\psi\cos\phi + \sin\psi\sin\theta\sin\phi & -\cos\psi\sin\phi + \sin\psi\sin\theta\cos\phi \\ \cos\psi\cos\theta & -\sin\psi\cos\phi + \cos\psi\sin\theta\sin\phi & \sin\psi\sin\phi + \cos\psi\sin\theta\cos\phi \\ \sin\theta & -\cos\theta\sin\phi & -\cos\theta\cos\phi \end{pmatrix}$$

The aircraft velocity vector in the ACRS, $\vec{\boldsymbol{V}}_{\boldsymbol{a}} = (V_{ax}, V_{ay}, V_{az})$, is then $\vec{\boldsymbol{V}}_{\boldsymbol{a}} = \mathbf{T}\vec{\boldsymbol{V}}_{\boldsymbol{a}'}$, where $\vec{\boldsymbol{V}}_{\boldsymbol{a}'}$ is the aircraft velocity vector with respect to FGRS. $\boldsymbol{V}_{\boldsymbol{a}'} = (V_{ew}, V_{ns}, V_w)$, where V_{ew} is the east component, V_{ns} is the north component, and V_w is the up component of the aircraft ground velocity.

For a non-zero distance between the IMU (ACRS origin) and the radar antenna, the aircraft rotational velocity $\vec{\boldsymbol{\omega}}$ contributes to measured aircraft velocity $\vec{\boldsymbol{V}}_{\boldsymbol{p}}$ in the beam, where $\vec{\boldsymbol{V}}_{\boldsymbol{p}} = \vec{\boldsymbol{V}}_{\boldsymbol{a}} + \vec{\boldsymbol{\omega}} \times \vec{\boldsymbol{R}}$, $\vec{\boldsymbol{R}} = (R_x, R_y, R_z)$ is the distance vector, and $\vec{\boldsymbol{\omega}} \times \vec{\boldsymbol{R}}$ is the radar arm moment. The aircraft attitude angles, body axis rotation rates, $\vec{\boldsymbol{\omega}}$, and the ground-referenced aircraft velocity vector $\boldsymbol{V}_{\boldsymbol{a}'}$ are obtained from the GNSS/IMU. The radar measured Doppler velocity for a given range gate is then

$$\boldsymbol{v} = \vec{\boldsymbol{b}} \cdot (\vec{\boldsymbol{V}}_{\boldsymbol{s}} + \mathbf{T}\vec{\boldsymbol{V}}_{\boldsymbol{a}'} + \vec{\boldsymbol{\omega}} \times \vec{\boldsymbol{R}})$$

where $\vec{\boldsymbol{V}}_{\boldsymbol{s}}$ is the target velocity. When the Doppler return is from stationary earth surface only, $\vec{\boldsymbol{V}}_{\boldsymbol{s}}$ is zero and the Doppler velocity becomes

$$\boldsymbol{v} = \vec{\boldsymbol{b}} \cdot \vec{\boldsymbol{V}}_{\boldsymbol{p}} = \vec{\boldsymbol{b}} \cdot (\mathbf{T}\vec{\boldsymbol{V}}_{\boldsymbol{a}'} + \vec{\boldsymbol{\omega}} \times \vec{\boldsymbol{R}}) \qquad (1)$$

The unknown quantity is the beam-pointing vector $\vec{\boldsymbol{b}}$. We obtain many observations of the surface Doppler velocity, and the scalar form of eq.(1) becomes

$$V_{px}^i b_x + V_{py}^i b_y + V_{pz}^i b_z = v^i \,,\ i = 1,2,\ldots,N, \qquad (2')$$

$$\sqrt{b_x^2 + b_y^2 + b_z^2} = 1, \qquad (2'')$$

where N is the number of measurements and the system coefficients V_{px}, V_{py} and V_{pz} for each measurement i are given by

$$\begin{aligned} V_{px} &= t_{11}V_{ew} + t_{12}V_{ns} + t_{13}V_w + V_{R1}; \quad V_{R1} = R_z\omega_y - R_y\omega_z \\ V_{py} &= t_{21}V_{ew} + t_{22}V_{ns} + t_{23}V_w + V_{R2}; \quad V_{R2} = R_x\omega_z - R_z\omega_x \\ V_{pz} &= t_{31}V_{ew} + t_{32}V_{ns} + t_{33}V_w + V_{R3}; \quad V_{R3} = R_y\omega_x - R_x\omega_y \end{aligned}$$

The beam vector components b_x, b_y, b_z are the unknowns and system (2) defines the beam calibration problem.

3. Calibration procedure

The calibration procedure is organized in three steps: (i) radar data is collected from carefully designed calibration flights, (ii) the data is divided into independent data segments (calibration legs) and for each calibration leg a numerical optimization procedure is run to solve the system (2), and (iii) a statistical analysis is performed to establish the beam-pointing calibration coefficients and their uncertainty.

3.1 *Aircraft beam calibration maneuvers and radar parameters*

The aircraft beam calibration maneuvers are designed to enhance the aircraft motion contribution into the radar antenna beam with respect to the ACRS axes and thus increase the robustness of the solution of (2). The maneuvers include aircraft

attitude angles typically encountered in research flight patterns. They are also designed to provide strong and unperturbed returns from the ground.

The calibration legs consist of short (~2 mins) straight and level legs with different angles between the aircraft heading and the mean wind direction and varying aircraft side-slip angle $\beta = \tan^{-1}\frac{V_{ay}}{V_{ax}}$

The calibration calculations involve solving the non-linear system (2) for each calibration leg. The left side of system (2) is affected by small navigation errors and 2nd order non-linearity. The navigation errors have weak effect on the system coefficients (V_{px}^i, V_{py}^i, V_{pz}^i). We used non-linear least square minimization software to solve (2).

4. Beam-pointing calibration results

The results for $b_x, b_y,$ and b_z from the solver of (2) for all 44 calibration legs are shown in Fig. 2. The left 3 panels are for the down antenna and the right 3 panels are for the down-forward antenna.

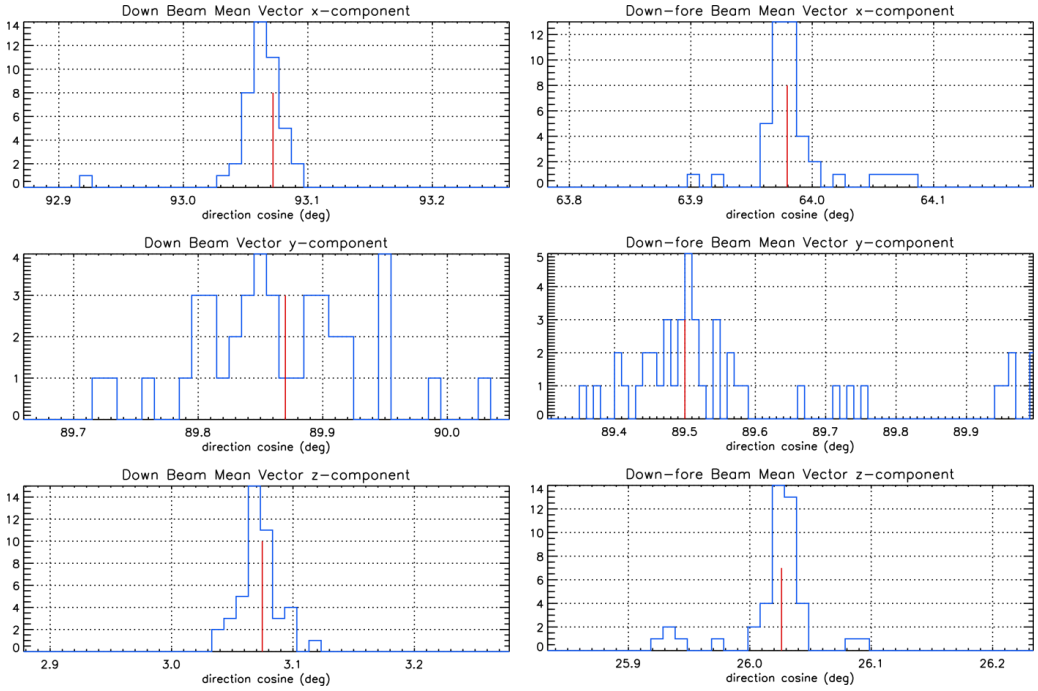

Fig. 2. Histograms of the antenna beam-pointing unit vector components b_x, b_y, b_z for the WCR down-pointing antenna (left panels) and down-forward pointing antenna (right panels). The beam components are plotted as directional arccosines of b_x, b_y, b_z in degrees. The red lines show the selected values for the final calibrated mean beam-pointing direction for both antennas.

The histograms in Fig. 2 are very narrow for the x- and z-components of the two beams with standard deviation of about 0.02˚ for the down beam, and about 0.03˚ for the down-forward beam. However, for the y-component of the beams, the histograms are quite broad with 0.14˚ and 0.18˚ standard deviations for the down and down-forward beams, respectively. There are a few outliers in the x- and z-component histograms, which are statistically less significant. The two WCR antennas analyzed here are designed to align their beams in a vertical plane parallel to the aircraft longitudinal axis. Typical maximum values for the velocity component V_{py} do not exceed 5 to 10 ms^{-1} for the calibration legs. For a deviation of b_y directional cosine by less than 0.5˚ from 90˚, the contribution of the V_{py} component of the platform motion into the beam is less than 0.09 ms^{-1}. This is comparable to the noise in the Doppler measurements and therefore it is to be expected that the solution for b_y is not very accurate. It would be more accurate to determine b_y using the mean values for b_x, b_z and solve (2") for b_y. Ten outliers deviate more than 0.05˚ from the center of the main lobes in the histograms for b_x and b_z. Nine of them are generated by the solutions for some of the straight flight calibration legs and 8 of them from straight legs flown in close alignment with the mean wind direction (type 1 in Table 2). In addition, the air vertical speed perturbations for these legs are also small. Thus the main contribution of the platform motion into the beams is mostly driven by the V_{ax}. Further simulation analysis (not shown) confirmed that the outliers result from erroneous solutions of (2). These legs were removed from the statistical analysis. The final results for the calibration coefficients and their uncertainties are shown in Table 2.

Table 2. WCR antenna beam-pointing unit vector in ACRS

WCR antenna	$cos^{-1}\,\boldsymbol{b_x}$		$cos^{-1}\,\boldsymbol{b_y}$		$cos^{-1}\,\boldsymbol{b_z}$		δ_b*
pointing beam	mean	st.dev.	mean	st.dev.	mean	st.dev.	
Down	93.072˚	0.011˚	89.870˚	0.017˚	3.075˚	0.013˚	0.021˚
Down-forward	63.979˚	0.008˚	89.488˚	0.011˚	26.026˚	0.008˚	0.016˚

* maximum beam-pointing angle error for one standard deviation error in b_x, b_y, b_z

5. Calibration evaluation

An example of the achieved accuracy of the retrieved velocity of the ground using the calibrated beam vectors for the down- and down-forward antennas is shown in Fig. 3.

The calibrated down and down-forward antenna beam unit vectors given in Table 2 are also tested using the surface data from all calibration flights. The calibration legs used in the beam vectors estimation represent about 27% of the data. The weather conditions for these flights were near optimal. The largest uncertainties in the variability of the radar Doppler measurements of the surface come from non-optimal surface conditions mainly from data outside the calibration legs. Fig. 4 shows the distributions of the residual velocity of the ground in the corrected radar Doppler measurements. Data from more than 5 hours of flying time is included, providing around 350000 radar profiles with surface returns. The absolute mean velocity of the ground does not exceed 0.01 ms^{-1} and the standard deviation is less than 0.1 ms^{-1}. These results are comparable to the mean and the standard deviation calculated for each of the calibration legs.

A separate analysis was performed to investigate the impact of large pressure differential between the aircraft cabin pressure and outside pressure. The effect is small for both down-pointing antennas and the bias in the velocity of the ground is mostly less than 0.1 ms^{-1} even for the rare UWKA cases when the pressure differential exceeds 350 hPa.

The antenna-pointing calibration coefficients from Table 2 were used for correcting the WCR Doppler data measurements recorded during ASCII experiment from January to March 2012 (http://flights.uwyo.edu/projects/ascii12). Nearly 50 hours of surface data were processed. The results confirmed the high accuracy of the aircraft motion correction and the applicability of using a single set of calibration coefficients for a given radar installation on the UWKA.

6. Conclusions

The WCR two down-pointing antennas on UWKA have narrow uncertainty envelopes and the rms error in the calibrated down and down-forward beams is smaller than 0.03°. The accuracy of the removal of the aircraft motion contribution from the radar Doppler data is better than 0.1 ms^{-1} and the uncertainty is less than 0.2 ms^{-1}. It should be noted that small systematic errors in the GNSS/IMU measurements could slightly bias the beam angle estimates from the calibration, but this is of no consequence to the error in the along-beam velocity corrections. The described calibration procedure is expected to be applicable to airborne Doppler radars with fixed-mounted (mechanically non-rotating) antennas installed on other aircraft. Higher accuracy of removing the aircraft motion contribution may be achieved by using a radar dedicated GNSS/IMU system mounted in close proximity to the antenna phase center, thereby eliminating uncertainty caused by the moment arm correction. This might be a necessary step for radars installed on aircraft subject to larger distortion in the airframe and large moment arm distances.

Acknowledgment

This work was supported by the NSF-University of Wyoming Cooperative Agreement AGS-0334908. The authors are in debt to the UWKA facility staff and especially the pilots who did an excellent job during the calibration flights. We are also thankful to Dr. Andrew Pazmany for the useful discussions during the course of this research.

References

Barton, D., Ward, H.R., 1984: *Handbook of radar measurement*, Artech House, 426 pp.

Bosart, B.L., Lee W. C., Wakimot,o R. M., 2002: Procedures to Improve the Accuracy of Airborne Doppler Radar Data. *J. Atmos. Oceanic Technol.*, **19,** 322–339.

Damiani, R., Haimov S., 2006: A High Resolution Dual-Doppler Technique for Fixed Multiantenna Airborne Radar. *IEEE Trans. Geoscience and Remote Sensing*, **44**, 3475-3489.

Kobayashi, S., Kumagai, H., 2003: Doppler velocity from sea surface on the spaceborne and airborne weather radars. *J. Atmos. Oceanic Technol.*, **20,** 372–381.

Lee, W.-C., Dodge, P., Marks, F. D., and Hildebrand, P. H., 1994: Mapping of airborne Doppler radar data. *J. Atmos. Oceanic Technol.*, **11,** 572–578.

Leon, D., Vali G., and Lothon, M., 2006: Dual-Doppler analysis in a single plane from an airborne platform. Part I: Technique. *J. Atmos. Oceanic. Technol.*, **23**, 3-21.

Wang, Z., French, J., Vali, G., Wechsler, P.J., Haimov, S., Rodi, A.R., Deng, M., Leon, D., Snider, J.R., Peng, L., Pazmany, A., 2012: Single aircraft integration of remote sensing and in situ sampling for the study of cloud microphysics and dynamics. *Bull. Amer. Meteor. Soc.*, **93** ,5, 653-668.

Skolnik, M., 2008: *Radar Handbook*, 3rd ed., McGraw-Hill, 1200 pp.